Georgia State University

ScholarWorks @ Georgia State University

Physics and Astronomy Theses

Department of Physics and Astronomy

8-8-2005

# New Correlation Effects in Nonrelativistic Atomic Photoionization in the High Energy Limit

Chieh Jen Yang

Follow this and additional works at: https://scholarworks.gsu.edu/phy_astr_theses

 Part of the Astrophysics and Astronomy Commons, and the Physics Commons

## Recommended Citation

Yang, Chieh Jen, "New Correlation Effects in Nonrelativistic Atomic Photoionization in the High Energy Limit." Thesis, Georgia State University, 2005.
https://scholarworks.gsu.edu/phy_astr_theses/1

This Thesis is brought to you for free and open access by the Department of Physics and Astronomy at ScholarWorks @ Georgia State University. It has been accepted for inclusion in Physics and Astronomy Theses by an authorized administrator of ScholarWorks @ Georgia State University. For more information, please contact scholarworks@gsu.edu.

**NEW CORRELATION EFFECTS IN NONRELATIVISIC ATOMIC PHOTOIONIZATION IN THE HIGH ENERGY LIMIT**

**by**

**CHIEH JEN YANG**

**Under direction of: STEVEN T. MANSON**

## Abstract

The effect of initial state correlation on high-energy dipole photoionization is considered and it is shown that for almost all atomic electron the asymptotic high-energy dependence is $E^{-7/2}$, and the dominant transition is an ionization plus excitation satellite transition. This is demonstrated in numerical calculations of the photoionization of Ge $4p^2\ ^1S$ and Sn $5p^2\ ^1S$.

# NEW CORRELATION EFFECTS IN NONRELATIVISIC ATOMIC PHOTOIONIZATION IN THE HIGH ENERGY LIMIT

**by**

**CHIEH JEN YANG**

A Thesis Submitted in Partial Fulfillment of the Requirements for the
Degree of Master in Science
in the College of Arts and Sciences
Georgia State University

2005

**NEW CORRELATION EFFECTS IN NONRELATIVISIC ATOMIC**

**PHOTOIONIZATION IN THE HIGH ENERGY LIMIT**

**by**

**CHIEH JEN YANG**

Major Professor: Steven T. Manson
Committee: William H. Nelson
He Xiaochun

Electronic Version Approved:

Office of Graduate Studies
College of Art and Sciences
Georgia State University
July 2005

# ACKNOWLEDGEMENTS

First, I would like to thank my thesis advisor, Dr. Manson for his teaching and revising this thesis, and everything he has done for me. I also like to thank Dr. Zhou for her help in the code running and Dr. Perera for his guidance and help. I would like to thank my two partners in the same group, Mr. Sossah and Mr. Chu for valuable discussion. Finally, I would like to express my deep appreciation to my committee members, Dr. Nelson and Dr. He for their wise suggestions and discussions.

# Table of Contents

**LIST OF FIGURES**

## 1. Introduction

Atomic physics is the fundamental starting point for many fields in physics. From a macroscopic viewpoint, atoms can be treated as the basic content of matter, and the properties of atoms are needed in order to construct the full picture of matter. The interaction between atoms and electromagnetic fields is very important and has been studied for a long time. We know that the electromagnetic field actually consists of photons. When an atom absorbs a photon it changes state, and the probability for the transition is related to a dimensionless quantity- oscillator strength. From oscillator strengths, oscillator strength moments can be defined. [1] Sums of moments of nonrelativistic oscillator strengths can be used to calculate a variety of atomic properties. Although at high energy the oscillator strength decreases with energy, for some cases these sums still need to go to a very high energy to be reasonably accurate. And for these cases it is very important to know the asymptotic behavior of oscillator strength in the high energy limit. The oscillator strength and therefore its moments are related to dipole approximation for photoabsorption. It was once thought that in high energy limit, the interaction between electrons will become unimportant, and the dipole matrix can be accurately evaluated by using single

particle wave functions. However, as recent results have pointed out [2,3], interchannel coupling remains important even at high energies, and data obtained via single particle approximation can be very wrong. Therefore, a new approach to oscillator strengths in the high energy range is needed, and this is the purpose of present work. Here we extend the analysis of previous work using both theory and numerical calculation.

In order to better elaborate the idea, note that the oscillator strength is defined as

$$f_{ka} = \frac{2m\omega_{ka}}{3\hbar}|\mathrm{r}_{ka}|^2$$

for a transition from state "a" to state "k", where $\omega_{ka} = \frac{E_k - E_a}{\hbar}$ and $\mathbf{r}_{ka}$ is matrix element of $\mathbf{r}, < k \mid \vec{r} \mid a >$. Interchannel coupling causes a change in the matrix element $\mathbf{r}_{ka}$, and, as a result, the oscillator strength at high energy is modified. This modification is important because in calculating atomic and molecular properties it is required to know the oscillator strength distributions from the lowest excitation to infinite energy. Actually, it was shown [1] that 40% of the sum comes from photon energy E>8 keV for one of the sum rules. When the photon energy is greater than the ionization energy, the excited electron goes into a continuum state, i.e., the case of photoionization. The dipole photoionization cross section is just proportional to the oscillator strength. (The cross section $\sigma_{ka} = \frac{4\pi^2\alpha\hbar^2}{m^2\omega_{ka}} | M_{ka} |^2$, where $M_{ka} = -\frac{m\omega_{ka}}{\hbar}\hat{\varepsilon}\cdot \mathrm{r}_{ka}$ is the dipole matrix element, so that it follows that $\sigma_{ka} = \frac{4\pi^2\alpha\hbar^2}{m^2\omega_{ka}} \frac{m^2\omega_{ka}^{\ 2}}{\hbar^2} | \mathrm{r}_{ka} |^2 = 4\pi^2\alpha\omega_{ka} | \mathrm{r}_{ka} |^2$ ,

so $\sigma_{ka} = \frac{6\pi^2 \alpha \hbar}{m} f_{ka}$, where $\alpha$ is the fine structure constant.) Owing to this proportionality, the sum of oscillator strengths can be used to check the consistency of measured and calculated photoionization cross sections.

In practice we use numerical methods to solve the problem, so why we are especially interested in obtaining a theoretical asymptotic formula for high energy? Why not just use numerical methods all the way and which will give not only asymptotic, but exactly answers for all energy if the calculation is correct? The reason is that due to the limitation of computer memory we are not able to do that. It is true that for low energy we can use numerical methods to obtain the cross section. However, for high energy, the photoelectron wave function oscillates very rapidly and requires extremely small mesh size to evaluate the numerical integral, and this generates numerical errors. For example, in this thesis we use nearly one million mesh points in our calculation (which is the best our machine can do), and it is just barely enough to obtain an accurate result. Therefore, a theoretical derivation for the high energy nonrelativistic atomic cross section is necessary.

A general asymptotic formula for the high energy atomic photoionization cross section has been obtained by Fano & Rao[4] using single-particle wave functions, which shows that the photoionization of an *nl* atomic electron falls off as $E^{(-7/2+l)}$ at asymptotically high energy.

However, the true wave function of a general atom can be written as a summation over a complete set; a linear combination of all possible configurations. This makes possible transitions from the initial state to many possible final states. The result of adding electron-electron correlation to the single-particle approximation in the form of interchannel coupling for high energy atomic photoionization showed that the cross section for an *nl* state ($l \neq 0$) behaves as $E^{(-9/2)}$ instead of $E^{(-7/2+l)}$ asymptotically [3]. Moreover, if we use multi-configuration initial state wave functions in calculation to include the effects of initial state correlation, then using the same logic, one can imagine this will affect the result too. In this thesis, we show that correlation in the form of initial state configuration interaction induces a further dramatic change in the high energy behavior of the photoionization cross section. Specifically, the photoionization cross section of all closed and almost all open subshells throughout the periodic table behaves as $E^{(-7/2)}$. In addition, for almost all $l \neq 0$ subshells, the dominant transition at high energy is photoionization plus excitation, a two-electron satellite transition. We also indicate that certain type of initial-state configurations cannot be ignored when evaluating the high energy photoionization cross section no matter how small its mixing in the initial wave function is. This is also useful when one needs to decide which configurations should be taken into account in particular cases, since as a practical matter, it is impossible to take an infinite number of

configurations into account.

This thesis is divided into four parts: Theory, Method of Calculation, Calculated Results and Conclusion. The Theory consists of four parts: Discussion of the dipole approximation and its limitations, the general single-particle high energy result of Rau & Fano, the changes in high energy behavior induced by interchannel coupling, and finally, the new idea of this thesis, we give the derivation of the effects of initial state configuration interaction. In the Method of Calculation section, we discuss how the numerical results have been obtained. This section also has four parts: Discrete state Hatree-Fock method; Discrete state multi-configuration Hartree-Fock method; Continuum wave calculation; and Length and velocity formulations. In the Calculated Results section, we give two examples of the nonrelativistic high energy photoionization cross section which are photoionization of outer $np^2\ ^1S$ subshells of Ge and Sn. In addition, the comparison of main and satellite lines is presented and discussed in this section.

## 2. Theory

### 2.1 Dipole Approximation

The origin of dipole approximation comes from time-dependant perturbation theory. Here we take the hydrogenic case as an example to illustrate the derivation, and using the same logic one can extend the result to the general case. For an atom in an electromagnetic field, in the Schrödinger equation momentum P must be replaced by P+e**A**. This gives

$$i\hbar \frac{\partial \psi}{\partial t} = \{-\frac{\hbar^2}{2m}\nabla^2 - \frac{Ze^2}{4\pi\varepsilon r} - i\hbar\frac{e}{m}\mathbf{A}\cdot\nabla + \frac{e^2\mathbf{A}^2}{2m}\}\psi \quad , \qquad (2.1.1)$$

and $\mathbf{A}=\int A_0(\omega)\hat{\varepsilon}[e^{i(\vec{k}\vec{r}-wt+\delta_\omega)}+e^{-i(\vec{k}\vec{r}-wt+\delta_\omega)}]d\omega$.

$-\frac{\hbar^2}{2m}\nabla^2-\frac{Ze^2}{4\pi\varepsilon r}$ represents the Hamiltonian of an electron in coulomb potential, and $-i\hbar\frac{e}{m}\mathbf{A}\cdot\nabla+\frac{e^2\mathbf{A}^2}{2m}$ are the perturbation terms. The term $\frac{e^2\mathbf{A}^2}{2m}$ includes $\mathbf{A}^2$ and if the field strength is small, $\mathbf{A}^2$ is quite small compared to **A**, and this term can be neglected. Thus the remaining perturbation term is $-i\hbar\frac{e}{m}\mathbf{A}\cdot\nabla$, and the magnitude of **A** depends on the density of photons. In the very low photon density limit, the situation will be well approximated by the first order time-dependent perturbation result, and this is the case we interested in. We obtain the result of first order time-dependent perturbation theory by the following way.

In Eq. (2.1.1), define the first two terms on the right hand side as $H_0$, and the solution for this Hamiltonian is the hydrogenic wave function, $\varphi_k$ ; $H_0 \varphi_k = E_k \varphi_k$.

We note that the solution for (2.1.1) can be express by a linear combination of hydrogenic functions,

$$\psi(\mathbf{r},t) = \sum_{\kappa} C_k(t)\varphi_\kappa(\mathbf{r})e^{\frac{-iEkt}{\hbar}} \quad . (2.1.2)$$

Substituting (2.1.2) into (2.1.1),

$$i\hbar\sum_k \dot{C}_k\varphi_\kappa(\mathbf{r})e^{\frac{-iEkt}{\hbar}} + \sum_k E_k C_k\varphi_\kappa(\mathbf{r})e^{\frac{-iEkt}{\hbar}} = \sum_k E_k C_k\varphi_\kappa(\mathbf{r})e^{\frac{-iEkt}{\hbar}} - \frac{i\hbar e}{m}\sum_k C_k e^{\frac{-iEkt}{\hbar}}(\mathbf{A}\cdot\nabla)\varphi_\kappa$$

$$\Rightarrow \quad i\hbar\sum_k \dot{C}_k\varphi_\kappa(\mathbf{r})e^{\frac{-iEkt}{\hbar}} = -\frac{i\hbar e}{m}\sum_k C_k e^{\frac{-iEkt}{\hbar}}(\mathbf{A}\cdot\nabla)\varphi_\kappa \quad .$$

Multipling both sides by $\varphi_b$* and integrating yields

$$\dot{C}_b = -\frac{e}{m}\sum_k C_k e^{\frac{i(E_b-E_k)t}{\hbar}} < \varphi_b \mid \mathbf{A}\cdot\nabla \mid \varphi_\kappa >$$

$$\Rightarrow \quad C_b = -\frac{e}{m}\int_0^t e^{i\omega_{ba}t} < \varphi_b \mid \mathbf{A}\cdot\nabla \mid \varphi_a > dt \quad , \quad (2.1.3)$$

where $\omega_{ba} = \frac{E_b - E_a}{\hbar}$.

Taking the absolute square of equation (2.1.3) gives the probability of transition from initial state "a" to final state "b". After evaluating the integral in (2.1.3) we get,

$$|C_k(t)|^2 \simeq 2\pi\frac{e^2A_0^2}{m^2}|M_{ba}(\omega_{ba})|^2\, t, \qquad \text{where } M_{ba} = < \varphi_b \mid e^{i\vec{k}\cdot\vec{r}}\hat{\varepsilon}\cdot\nabla \mid \varphi_a > \quad .$$

The transition rate $W_{ba}$ is then given by,

$$W_{ba} = 2\pi\frac{e^2A_0^2}{m^2}|M_{ba}(\omega_{ba})|^2 . \quad (2.1.4)$$

From the transition rate we can calculate the oscillator strengths and cross section.

One difficulty in evaluating (2.1.4) comes from the matrix element $M_{ba}$. It contains the term $e^{i\vec{k}\cdot\vec{r}}$ which represents the photon plane wave. In the low energy case, which means k is small, we can make an approximation called the dipole approximation.

Since $kr \sim \frac{E}{\hbar c}\frac{\hbar^2}{me^2} = E\frac{\hbar}{mce^2} \sim E\cdot 10^{-4}$ (E is in units of Rydbergs) for a medium size atom, we can expand $e^{i\vec{k}\vec{r}} = 1 + i\vec{k}\cdot\vec{r} + ....$ and approximate it as 1 when the energy of the photon is small. The physical meaning for this approximation is that the wave length of photon is much longer than the size of an atom. Of course, for very high energy photons, dipole approximation will no longer be valid. However, since many properties of atoms, like the various sum rules, can be calculated in terms of dipole oscillator strength, it is of interest to study the dipole matrix element even in energy regions where it is not directly applicable to transitions. Furthermore, the asymptotic high-energy dipole photoionization cross section (oscillator strength) is an interesting and much-studied question in itself.

## 2.2 General single-particle high energy result

In 1967, Rau and Fano evaluated the behavior of the inelastic scattering form factor in high energy region [4]. The form factor is given by:

$$\int \psi_f^* \sum_j \exp(i\vec{q}\cdot\vec{r}_j)\psi_i dr \text{ , (2.2.1)}$$

where $\vec{q}$ is the momentum transfer. Note that this form factor is similar in form as the matrix element for photoionization, $M_{ba}$, except for photoionization there is a gradient in the transition operator in the matrix element.

The methodology of Ref.[4] is to expand $\exp(i\vec{q}\cdot\vec{r}_j)$ in a sum of products of Legendre polynomials, $P_L(\cos\theta)$ and spherical Bessel functions, $j_L(qr)$,

$$j_L(qr) = [\frac{\pi}{2qr}]^{1/2} J_{L+1/2}(qr) .$$

Plugging this into the integral in (2.2.1) yields a sum of products of the radial parts (2.2.2) and angular part (2.2.3),

$$\int_0^\infty R_{kl'}(r)\, j_L(qr) R_{nl}(r) r^2 dr , \quad \text{(2.2.2)}$$

$$\int Y_{l'm'}{}^* P_L(\cos\theta) Y_{lm} d\Omega , \qquad \text{(2.2.3)}$$

where L varies from |*l*-*l'*| to *l*+*l'*. The integral of (2.2.3) is related to the parity selection rule and the triangular condition, which gives further constraints to the value of L (L=1,3,5,…). To evaluate (2.2.2), note that if q is very large, the Bessel function oscillates very rapidly except at *r* near the origin, and the larger the q is, the smaller this region around the origin is. It is clear that integral (2.2.2) decreases with energy due to the smaller region near the origin. The rapid oscillation of the spherical Bessel function outside this region causes cancellation in outer region,

so that the main contribution to the integral, (2.2.2), arises from the region of small values of r, and the bigger the q is, the smaller this region is. To evaluate the explicit relationship, we expand the radial parts of the wave functions in a power series in r,

$$R_{nl} = b_0 r^l + b_1 r^{l+1} + .... \quad , (2.2.4)$$

$$R_{kl'} = f_0 r^{l'} + f_1 r^{l'+1} + ...., (2.2.5)$$

Then the integral (2.2.2) becomes:

$$\int_0^\infty (f_0 r^{l'} + f_1 r^{l'+1} + ...) j_L(qr)(b_0 r^l + b_1 r^{l+1} + ...) r^2 dr$$

$$= \int f_0 b_0 r^{l'+l+2} j_L(qr) dr + \int (f_0 b_1 + f_1 b_0) r^{l'+l+3} j_L(qr) dr + \int (f_0 b_2 + f_1 b_1 + f_2 b_0) r^{l'+l+4} j_L(qr) dr + ...$$

$$= \sum_s C_s \int_0^\infty r^{l+l'+2+s} j_L(qr) dr \quad , (2.2.6)$$

with $C_s \equiv \sum_{i \le s} f_i b_{s-i}$ .

To evaluate (2.2.6), we use [5],

$$\int_0^\infty r^b J_a(qr) dr = 2^b q^{-b-1} \Gamma[\frac{1}{2}(a+b+1)] / \Gamma[\frac{1}{2}(a-b+1)] \quad ,$$

with the conditions Re(a+b)>-1 and Re(b)<1/2 (Re means real part). The latter condition is not fulfilled in our case. However, we can still use this formula in the following manner. We factor out of Eq. (2.2.6) $\exp(-\varepsilon r)$ , so it becomes

$$\int_0^\infty e^{-\varepsilon r} r^{l+l'+2+s} j_L(qr)dr \text{ , (2.2.7)}$$

where $\varepsilon$ is a small positive number. This allows us to apply Eq.(3), Sec. 13.2 of Ref.5, which states that the value of (2.2.7) is proportional to

$$F(\frac{1}{2}[l+l'+L+3+s), \frac{1}{2}[L-l-l'-2-s], L+\frac{3}{2}, q^2/[q^2+\varepsilon^2]) .$$

Applying the formula in the limit $\varepsilon \to 0$, the integral of (2.2.6) then is equal to

$$\sum_s C_s(\sqrt{\pi}) 2^{l+l'+1+s} q^{-(l+l'+3+s)} \cdot \Gamma[\frac{1}{2}(l+l'+L+3+s)] / \Gamma[\frac{1}{2}(L-l-l'-s)] . \text{ (2.2.8)}$$

From (2.2.8), since we are interested in very large q, we can take the lowest order non-vanishing term in (1/q). In this way the general dependence of q is obtained. Since $\Gamma(x)$ equals to an infinite complex number if x is a negative integer, and the angular integral, Eq.(2.2.3), will be non-zero only if the value of $L-l'-l$ is even (parity selection rule) and $L-l'-l \le 0$ (triangular condition), so all terms with even s vanish in Eq.(2.2.8) (because this makes the argument of the $\Gamma$ function in the denominator a negative integer). As a result, the leading term of (2.2.8) is determined by s=1 and is $q^{-(l+l'+4)}$, for $q \to \infty$.

Similarly, for high energy photoionization case the radial part of the continuum wave $R_{kl'}$ can be expressed as

$$R_{kl'}(r) \sim N_k j_{l'}(kr)$$

with normalization factor $N_k = [2mk/\pi\hbar^2]^{1/2}$.

For our case, atomic photoionization, the dipole matrix element is given by

$$M = \int_0^\infty R_{kl'}(r)\nabla R_{nl}(r)r^2 dr .$$

Since $\nabla = \frac{i}{\hbar}P$,

$$M = \int_0^\infty R_{kl'}(r)\nabla R_{nl}(r)r^2 dr$$

$$= \int_0^\infty R_{kl'}(r)(\frac{i}{\hbar}P)R_{nl}(r)r^2 dr$$

$$\sim \int_0^\infty [2mk/\pi\hbar^2]^{1/2} j_{l'}(kr)(P)R_{nl}(r)r^2 dr$$

$$\sim \int_0^\infty [2mk/\pi\hbar^2]^{1/2} j_{l'}(kr)(P)(b_0 r^l + b_1 r^{l+1} + ...)r^2 dr$$

$$\sim O[Pk^{1/2}\int_0^\infty j_{l'}(kr)r^{l+s+2}dr]$$

(Where $s = 0,1,2,3....$ and play the same role as in (2.7))

$$\sim O[Pk^{1/2}k^{-(l+s+3)}\Gamma(\frac{1}{2}(l'+l+s+2+1))/\Gamma(\frac{1}{2}(l'-l-s-2+1))] \quad . \qquad (2.2.9)$$

Again, since the argument of gamma function in dominator can't be negative integer or zero, and we note that for the case of dipole transition $l'-l = \pm 1$, so the lowest $s$ must be 1. Which ends up that the matrix element $M \sim O[Pk^{1/2}k^{-(l+4)}] \sim O[Pk^{-(l+7/2)}]$.

As a result, the cross section is

$$\sigma \sim \frac{1}{\Delta E}|M|^2$$

$$\sim \frac{P^2}{\Delta E}k^{-(l+7/2)\cdot 2} \quad (2.2.10)$$

$$\sim E^{-(l+7/2)} \quad .$$

We can cancel out $P^2$ with $\Delta E$ because P is the momentum of photon and its square is proportional to the energy transferred. We emphasize that is the asymptotic high energy dependence of dipole photoionization using single particle wave functions.

**2.3 Changes in high energy behavior induced by interchannel coupling**

As mentioned above, atomic wave functions can be accurately represented by linear combinations of single particle wave functions, both in the discrete and in the continuum. The above asymptotic result derived with single-particle wave functions is partially wrong, and we must include multi-configuration and interchannel coupling effects in order to correctly predict nature of the high energy asymptotic form. The effect of interchannel coupling on high-energy atomic photoionization cross section was derived several years ago [2]. For this derivation, it turns out to be most convenient to transform the problem into momentum space. The idea is the same as the derivation of previous section, but now we work in momentum space.

The effect of interchannel coupling can be treated in second order perturbation theory in the calculation of the dipole matrix element. The transition can be represented by Feynman diagrams as follows:

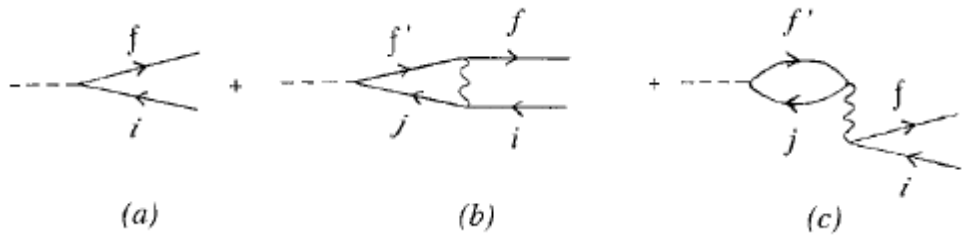


The first order term (Diagram (a)) is the single-particle dipole matrix element $d_{if} =< f \mid d \mid i >$.

The second order term is

$$\Delta D_{if}^{(2)}(\omega) = \lim_{\delta \to 0} \sum_{j \le F, f' > F} \frac{(j \mid \mathrm{d} \mid f')[(f'i \mid V \mid fj) - (f'i \mid V \mid jf)]}{\varepsilon_j - \varepsilon_{f'} + \omega + i\delta} \quad , (2.3.1)$$

where *V* is the coulomb potential between electrons and $\omega$ is the photon energy (for which we use E to represent in previous section). *j, f', f, i* represent the states as labeled in above diagrams, $\varepsilon_j - \varepsilon_{f'}$ is the energy difference between these two states. To illustrate, we consider $np \to \varepsilon k$ photoionization.

The first order, i.e. dipole matrix element is,

$$d_{np,\varepsilon\vec{k}} =< np \mid i\vec{e} \cdot \nabla \mid \varepsilon\vec{k} >= O((\vec{e} \cdot \vec{k})\tilde{\phi}_{np}(k)) \quad \text{(in momentum space).} \quad (2.3.2)$$

For a single-particle matrix element [4], we know that the cross section obtained from the dipole matrix element in Eq.(2.3.2) is of order $\frac{1}{\omega^{9/2}}$. Now, we estimate those terms in second order which have the same or bigger contribution asymptotically than first order. Note that in case (c), due to the smallness of $(f'i \mid V \mid jf)$, the second order matrix element falls off much faster with increasing k than first order. The physical reason is that the large energy transfer to the

intermediate states is not likely to happen. However, in case (b) the energy transfer is not big and the contribution to the matrix element needs to be included. To evaluate case (b), we separate the matrix element into real and imaginary parts. In momentum space, the real part and imaginary parts are

$$\mathrm{Re}\,\Delta D^{(2)}_{np,\varepsilon\vec{k}}(\omega) = \wp\int (\vec{e}\cdot\vec{k}')\frac{\tilde{\phi}_{n's}(k')}{k^2-k'^2}\frac{4\pi}{|\vec{k}-\vec{k}'|^2}(n's\,|\,e^{i(\vec{k}'-\vec{k})\cdot\vec{r}}\,|\,np)\frac{d\vec{k}'}{(2\pi)^3}, \quad (2.3.3)$$

$$\mathrm{Im}\,\Delta D^{(2)}_{np,\varepsilon\vec{k}}(\omega) = \frac{\pi}{2k}\int (\vec{e}\cdot\vec{k}')\tilde{\phi}_{n's}(k')\frac{4\pi}{|\vec{k}-\vec{k}'|^2}(n's\,|\,e^{i(\vec{k}'-\vec{k})\cdot\vec{r}}\,|\,np)\delta(k^2-k'^2)\frac{d\vec{k}'}{(2\pi)^3}. \quad (2.3.4)$$

In these expressions the plane waves have been normalized to unit amplitude, $\tilde{\phi}_{n's}(k')$ is the Fourier transform of wave function in momentum space, $\wp$ is the principal value. Also, in the sum over *j* we only retain the term *j=n's*, because, as discussed previously, the value of matrix element in form of $\langle n'l'|exp(iqr)|nl\rangle$ is proportion to $E^{-(9/2+l)}$, so the *s* state will be the dominant term.

Due to the form $\frac{e^{i(\vec{k}'-\vec{k})\cdot\vec{r}}}{|\vec{k}-\vec{k}'|^2}$ in the integral of (2.3.3), only when $\vec{k}'\sim\vec{k}$ will there be a significant contribution. Then we can expand (2.3.3) in powers of $\vec{k}'\sim\vec{k}$ and retain the lowest order. We consider Eq.(2.3.3) as a function $f(k')$, and $f(k') = f(k)+(k'-k)f'(k)+\ldots$, where we ignore the higher order terms because $\vec{k}'\sim\vec{k}$. The first term $f(k)$ vanishes, and the second term becomes

$$
\begin{aligned}
&(k-k')f'(k) \\
&= (k-k')(\vec{e}\cdot\vec{k}')\frac{\tilde{\phi}_{n's}(k')}{k^2-k'^2}\frac{4\pi}{|\vec{k}-\vec{k}'|^2}(n's\,|\,e^{i(\vec{k}'-\vec{k})\cdot\vec{r}}\,|\,np)\frac{1}{(2\pi)^3} \\
&= (\vec{e}\cdot\vec{k}')(k-k')\frac{\tilde{\phi}_{n's}(k')}{k^2-k'^2}\frac{4\pi}{|\vec{k}-\vec{k}'|^2}(n's\,|\,e^{i(\vec{k}'-\vec{k})\cdot\vec{r}}\,|\,np)\frac{1}{(2\pi)^3} \\
&\sim (\vec{e}\cdot\vec{k}')\frac{\tilde{\phi}_{n's}(k')(k-k')}{(k+k')(k-k')}\frac{1}{|\vec{k}-\vec{k}'|^2}(n's\,|\,e^{i(\vec{k}'-\vec{k})\cdot\vec{r}}\,|\,np) \\
&\sim (\vec{e}\cdot\vec{k}')\frac{\tilde{\phi}_{n's}(k')}{(k+k')q^2}(n's\,|\,e^{iq\cdot\vec{r}}\,|\,np) \\
&\sim O((\vec{e}\cdot\vec{k}')\frac{\tilde{\phi}_{n's}(k')}{k}) \quad ,
\end{aligned}
$$

(2.3.5)

where $q \equiv \vec{k}' - \vec{k}$, and the term $\tilde{\phi}_{n's}(k')$ is of order $k^0$ since for an "s" state, *l=0*. Thus $\frac{\tilde{\phi}_{n's}(k')}{k}$ is of order *1/k*, which is in the same order as $\tilde{\phi}_{np}(k)$ in Eq.(2.3.2). Therefore, the final result is that Eq.(2.3.5) has the same asymptotic energy, leading to a non-vanishing correction to the single particle amplitude in the limit of $\omega \to \infty$. For the imaginary part, since Eq.(2.3.4) has an extra factor of $\pi/2k$, the value will be smaller by a factor of *1/k* compare to the real part (Eq.(2.3.3)) and can be neglected as $k \to \infty$. It is important to note that the asymptotic energy dependence of the second order contribution to the dipole matrix element is independent of the outgoing electron. Thus for photoionization of an *nl* electron with *l>1*, the term will dominate the dipole matrix element asymptotically.

The conclusion is that for initial state *l=0*, the cross section will behave like $\omega^{-7/2}$ as predicted by Fano & Rau's formula; but for all *l>0* it will behave as $\omega^{-9/2}$ due to the

interchannel coupling.

## 2.4 Changes induced by initial state configuration interaction

From the previous discussion, we have obtained a general formula for dipole matrix element which accounts for the effects of interchannel coupling in the high energy limit. However, there is still one thing haven't been included so far; correlation in the initial discrete state which can be taken in account via configuration interaction. The effect of this initial state correlation in nonrelativistic atomic photoionization in high energy limit is the main result of this thesis. The correction due to initial state configuration interaction will be derived theoretically in the section. Examples calculated numerically will be presented in the later section.

The effect of initial state correlation can best be demonstrated by an example. Consider the outer $(3p)^6$ ground state of the Ar atom. Including initial state correlation with the $3p^4 4s^2\ ^1S$ configuration leads to a wave function of the form

$$|i\rangle = \alpha|3p^6\rangle + \beta|3p^4 4s^2\rangle, \qquad (2.4.1)$$

where the expansion coefficient $\alpha$ is close to unity, and $\beta << \alpha$. From this initial state, photoionizing transitions to the final states

$$|f_1\rangle = |3p^5\ \varepsilon s\rangle,\ |f_2\rangle = |3p^5\ \varepsilon d\rangle,\ |f_3\rangle = |3p^4 4s\ \varepsilon p\rangle \qquad (2.4.2a,b,c)$$

can occur. The cross section for leaving the $Ar^+$ in the $|3p^5>$ state, i.e., the single-particle transition, is then (in the dipole-length formulation) simply

$$\sigma(3p^5) = |\alpha|^2(h\nu)K[|<i|\Sigma\mathbf{r}_i|f_1>|^2 + |<i|\Sigma\mathbf{r}_i|f_2>|^2] = |\alpha|^2(h\nu)KQ[|<3p|\mathbf{r}|\ \varepsilon s>|^2 + |<3p|\mathbf{r}|\ \varepsilon d>|^2], \quad (2.4.3)$$

where hν is the photon energy, K is a universal constant, $\mathbf{r}_i$ is the position vector for the i-th target electron, and Q (of order unity) is the product of the overlap integrals of inactive electrons reflecting the fact that the orbitals differ somewhat in initial and final states. Except for the factors of Q and $|\alpha|^2$, both of order unity, Eq. (2.4.3) is identical to the single-particle expression for the photoionization of the $(3p)^6$ subshell. From the discussion of the previous paragraph then, it is clear that this cross section behaves asymptotically as $E^{-9/2}$. Similarly, the cross section for leaving the $Ar^+$ in the excited $|3p^4 4s>$ state is

$$\sigma(3p^4 4s) = |\beta|^2[|<i|\Sigma\mathbf{r}_i|f_3>|^2\ ] = |\beta|^2(h\nu)KQ'[|<4s|\mathbf{r}|\ \varepsilon p>|^2], \quad (2.4.4)$$

where Q' is the overlap factor (also of order unity) in this case. This cross section to the excited state differs from the cross section to the ground state in two important respects: First, the factor of $|\beta|^2$ is very much smaller than unity; second, and more important, is that except for the factors Q' and $|\beta|^2$, Eq. (2.4.4) is the expression for the single-particle cross section for photoionizing a 4*s* electron from a $3p^4 4s$ initial state. Thus, the discussion of the previous paragraph demonstrates that the asymptotic high energy behavior for this photoionization plus excitation

(satellite) cross section is $E^{-7/2}$. At low energy, where the dipole matrix element for both transitions are of the same order, $\sigma(3p^4 4s) << \sigma(3p^5)$ by a factor of order $|\beta|^2$ which, as discussed is very much smaller than unity, i.e., the inclusion of initial state correlation shows that photoionization plus excitation is very much less probable than the single particle photoionization process, as expected. However, no matter how small $|\beta|^2$ is, in the limit of asymptotically high energy, $\sigma(3p^4 4s)$, which falls off more slowly than $\sigma(3p^5)$ by a factor of E, must dominate. This leads to two dramatic consequences: The high energy limit of the photoabsorption cross section of the $(3p)^6$ subshell behaves as $E^{-7/2}$, not $E^{-9/2}$ as predicted on the basis of interchannel coupling [3]. In addition, in the limit of high energy, the two-electron photoionization plus excitation (satellite) cross section dominates over single-particle photoionization (main line) cross section. Both of these conclusions differ strikingly from the conventional wisdom.

It is of importance to point out the generality of these effects. From the example of the photoionization of the Ar $(3p)^6$ subshell, it is evident that the only condition required for this effect to be present for a particular subshell is that there exist configuration interaction of the configuration of the subshell with a configuration containing at least one ns electron. This is clearly possible for any closed subshell; $(nl)^{4l+2}$ can always be mixed with $(nl)^{4l}(n's)^2$.

Furthermore, *most* open-shell configurations can also be mixed. For example, $(np)^2\ ^1S$ can be mixed with $(n's)^2$, $(np)^2\ ^1D$ can be mixed with $(nd n's)\ ^1D$, etc. As a matter of fact, among the $(np)^q$ configurations, which yield 12 individual multiplets, only $np$, $(np)^2\ ^3P$, and $(np)^3\ ^4S$ *cannot* be mixed with configurations containing an $ns$ electron. Similar considerations apply to $(nd)^q$ and $(nf)^q$ configurations, along with systems with more than one open shell. Thus, the conclusions of the previous paragraph apply to almost all subshells of both ground and excited states of all of the atoms of the periodic system. In other words, the new high-energy phenomenology detailed above applies to all but a handful cases.

## 3. Method of Calculation

In the previous section the asymptotic form of the dipole photoionization cross section at high energy was derived. It is useful to demonstrate the effects described by explicit calculation. In this section we present the background and methodology for the calculations which employ Hartree-Fock and multi-configuration Hartree-Fock formulations.

### 3.1 Discrete state Hartree-Fock

The basic idea of the Hartree-Fock theory stems from the variational principle that says that the energy functional $<\phi|\mathrm{H}|\phi>$ will have local minimum in the vicinity of the eigenvalues of H, subject to the constraint that $\phi$ is normalized.

We use this idea to calculate the electron wave functions of a many electron atom. First, we write down the Hamiltonian of the whole system.

$$H=\sum_{i\neq j}(H_0+\frac{e^2}{r_{ij}}) \quad , \quad H_0=\sum_i(\frac{p_i^2}{2m}-\frac{Ze^2}{r_i}) . \quad (3.1.1)$$

The trial function is given as

$$\Phi = \frac{1}{\sqrt{N!}} \begin{vmatrix} \phi(1)_{1s\uparrow} & \phi(1)_{1s\downarrow} & \phi(1)_{2s\uparrow} & ....\phi(1)_n \\ \phi(2)_{1s\uparrow} & \phi(2)_{1s\downarrow} & .... & \\ \vdots & & & \\ \phi(n)_{1s\uparrow} & & & \end{vmatrix}$$

which is a Slater determinant. Substituting the Slater determinant in (3.1.1), <H> yields

$$< H >= \sum_i < \Phi \mid H_0 \mid \Phi > + \sum_{i<j} < \Phi \mid \frac{e^2}{r_{ij}} \mid \Phi >$$

$$= \sum_i (H_0(i))_{ii} + \sum_{i<j} (H_2)_{ij,ij} - \sum_{i<j} (H_2)_{ij,ji} \quad , \quad (\frac{e^2}{r_{ij}} \equiv H_2)$$

To obtain the wave functions of each orbital, we vary $< H >$ with Lagrange multipliers to include the constraint of orthogonally,

$$\delta(< H > + \lambda_{1s} < 1s \mid 1s > + ... + \lambda_{nl} < nl \mid nl > + \lambda_{1s,2s} < 1s \mid 2s > + ... + \lambda_{nl,n'l} < nl \mid n'l >) = 0$$

After varying <H> with respect to each orbital and perform the angular integrations specifically, we get the Hartree-Fock equations, which are a set of equations and each equation represents a particular sub-shell. The general form is

$$[\frac{d^2}{dr^2} - \frac{l(l+1)}{r^2} + \frac{2Z}{r} - \frac{2}{r}(D) - E_{nl}]P_{nl}(r) - \frac{2}{r}(X) = \sum_{n'} \lambda_{nl,n'l} P_{n'l}(r) \quad (3.1.2)$$

where D and X are the direct and exchange terms respectively,

$$\text{D} = \sum_{n'l'} \sum_k y_{nl,n'l'}(k) Y^k(n'l', n'l'; r),$$

$$\text{X} = \sum_{n'l'} \sum_k x_{nl,n'l'}(k) Y^k(nl, n'l'; r) P_{n'l}(r),$$

$y_{nl,n'l'}$ , $x_{nl,n'l'}$ are coefficients resulting from angular integrals. And

$$Y^k(nl,n'l';r)=\int_0^\infty P_{nl}(\frac{1}{r_{12}})P_{n'l'}dr=\frac{1}{r^{k+1}}\int_0^r P_{nl}(r')r'^k\,P_{n'l'}(r')dr'+r^k\int_r^\infty\frac{P_{nl}(r')P_{n'l'}(r')}{r'^{k+1}}dr'.$$

To solve the Hartree-Fock equations, we start with a trial function with hydrogenic orbits and iterate until all the orbitals converge. This calculation is done numerically. This form of differential equation is guaranteed to have a unique solution by a mathematical theory called the contract mapping principle.

### 3.2 Discrete state Multi-configuration Hartree-Fock

The result obtained above is the single configuration Hartree-Fock wave function. In many case the single configuration result is quite good. However, owing to the variantional principle, the result of the single configuration Hartree-Fock method can always be improved upon by using a multi-configuration wave function. Thus we take a wave function of the form $\Phi=\sum c_i\phi_i$, where each of the $\phi_i$ are Slater determinants as defined above. Then, with the constraint that $\sum|c_i|^2=1$ to insure normalization, the variation principle invoked leading to the multi-configuration Hartree-Fock equation.

### 3.3 Continuum Hartree-Fock

Since we are dealing with photoionization problem, in addition to discrete state, we need the wave function of the outgoing electron also. One can immediately infer that the way of getting

the wave function of outgoing electron is just the same as discrete case, because Hartree-Fock method doesn't specify or limited to which types of wave functions should be used. In equation (3.1.2), by replacing $P_{nl}$ with continue wave $P_{\varepsilon l}$ we can still solve the wave function. However, there is one problem- the normalization. The continuum is a non-normalizable wave functions; it is normalize on a $\delta$-function scale. In order to get the continue wave normalized, another theoretical approach must be employed. Defining the deviation $u(r)$ from the coulomb field in the Hartree-Fock equation for a continuum electron, $P_{\varepsilon l}$,

$$P''_{\varepsilon l}(r) + A(r)P_{\varepsilon l}(r) = 0 \qquad (3.3.1)$$

where $A(r) = u(r) + \frac{2}{r} + \varepsilon - \frac{l(l+1)}{r^2}$,

with limits on *u(r)*,

$$r \to \infty,\ u(r) \to 0.$$
$$r \to 0,\ u(r) \to \frac{2(Z-1)}{r}.$$

Equation (3.3.1) has normalized solution:

$$P_{\varepsilon l}(r) = (\pi x)^{-1/2} \sin\theta(r) \qquad (3.3.2)$$
$$where\ \ x = \theta'(r)$$

Substituting (3.3.2) into (3.3.1), we get:

$$x^2 = A(r) + x^{1/2}\frac{d}{dr^2}(x^{-1/2}) = A(r) + \frac{3}{4}\frac{x'^2}{x^2} - \frac{1}{2}\frac{x''}{x}$$

For $\varepsilon > 0$, and large enough r, $A = \varepsilon,$ and $x = \varepsilon^{1/2}, \theta = \varepsilon^{1/2} r + \delta$

So that $P_{\varepsilon l}(r) \xrightarrow[r\to\infty]{} \frac{1}{\pi^{1/2}\varepsilon^{1/4}} \sin(\varepsilon^{1/2} r + \delta)$ (3.3.3)

For $\varepsilon = 0$, and large enough r: $A = \frac{2}{r}$, $x = \sqrt{2/r}$, $\theta = \sqrt{8r} + \delta$

So that $P_{0l} \xrightarrow[r\to\infty]{} \frac{r^{1/4}}{\pi^{1/2} 2^{1/4}} \sin(\sqrt{8r} + \delta)$ (3.3.4)

From (3.3.3) and (3.3.4), we have the asymptotic wave function for the continuum state. So suppose $\overline{P}_{\varepsilon l}(r)$ is the un-normalized continuum wave obtained from the numerical solution of the Hartree-Fock equation; we can calculate the normalization constant C via dividing the numerical function by the analytic function (above) in the asymptotic region,

$$\overline{P}_{\varepsilon l}(r) / P_{\varepsilon l}(r) = C .$$

### 3.4 Length and Velocity Formulations

Now we have all the wave functions we need, the next step is to calculate the matrix element. The dipole matrix is given by

$$\begin{aligned} M_{ba} &= \hat{\varepsilon} \cdot < \Phi_b \mid \nabla \mid \Phi_a > \\ &= \frac{i}{\hbar} \hat{\varepsilon} \cdot < \Phi_b \mid \vec{P} \mid \Phi_a > \quad . \end{aligned} \tag{3.4.1}$$

Using the fact that

$$[H, \vec{r}] = -i\hbar \frac{\partial \vec{r}}{\partial t} = -\frac{i\hbar}{m} \vec{P}$$

So that $\vec{P} = \frac{im}{\hbar} [H, \vec{r}]$.

Substituting into (3.4.1) gives

$$M_{ba} = -\frac{m}{\hbar^2}\hat{\varepsilon}\cdot < \Phi_b \,|\, [H, \vec{r}\,] \,|\, \Phi_a >$$

$$= -\frac{m}{\hbar^2}\hat{\varepsilon}\cdot (E_b - E_a) < \Phi_b \,|\, \vec{r} \,|\, \Phi_a > \qquad (3.4.2)$$

$$= -\frac{m\omega_{ba}}{\hbar}\hat{\varepsilon}\cdot < \Phi_b \,|\, \vec{r} \,|\, \Phi_a > \quad .$$

The term $< \Phi_b \,|\, \vec{r} \,|\, \Phi_a >$ can be calculated by another way. From equation (3.4.1) and middle line of (3.4.2)

$$M_{ba} = \frac{i}{\hbar}\hat{\varepsilon}\cdot < \Phi_b \,|\, \vec{P} \,|\, \Phi_a >$$

$$= -\frac{m}{\hbar^2}\hat{\varepsilon}\cdot (E_b - E_a) < \Phi_b \,|\, \vec{r} \,|\, \Phi_a > \ ,$$

$$\therefore \quad < \Phi_b \,|\, \vec{r} \,|\, \Phi_a > = \frac{-1}{E_b - E_a}\frac{i\hbar}{m} < \Phi_b \,|\, \vec{P} \,|\, \Phi_a > = -\frac{i}{m\omega_{ba}} < \Phi_b \,|\, \vec{P} \,|\, \Phi_a > . \quad (3.4.3)$$

Normally we use $r_{ba}$ to represent $< \Phi_b \,|\, \vec{r} \,|\, \Phi_a >$, and $P_{ba}$ to represent $< \Phi_b \,|\, \vec{P} \,|\, \Phi_a >$. $r_{ba}$ is the so called dipole length matrix element, and $P_{ba}$ is the dipole velocity matrix element. The two formulations must give exactly the same result if the wave functions are exact. In numerical calculations, using approximate wave functions and comparing these two formulations' results give us an idea as to the accuracy of the calculation.

## 4. Calculated Results

In order to verify the general derivation, we have performed calculations on the photoionization of Ge $4p^2$ $^1$P and Sn $5p^2$ $^1$P. We have used the mchf (multiconfiguration Hartree-Fock) code developed by Charlotte Froese Fisher[6] to generate the initial states and ionic core wave functions for the cases of intends. Then we used our own photoionization code to calculate the continuum wave function and cross section. In each case we have considered the initial $np^2$ state configuration interaction with an $(n+1)s^2$ configuration, $5s^2$ for Ge and $6s^2$ for Sn. These cases were chosen because the coefficients of the $(n+1)s^2$ configuration, in each case are significant, 0.069 for Ge and 0.066 for Sn. Calculations were performed for photoionization to the *4p* and *5s* states of $Ge^+$, and the *5p* and *6s* states of $Sn^+$. The calculations were performed up to an energy of 90,000 Ryd in both length and velocity formulations.

The results of our calculation for Ge going to $Ge^+$ *4p* and *5s* in the energy range up to 1,000 Ryd are shown in FIGs. 1 and 2. For the photoionization to $Ge^+$ *4p,* final states $4p\varepsilon s$ and $4p\varepsilon d$ were considered, while for transitions to $Ge^+$*5s*, only the $5s\varepsilon p$ final state was necessary. Two points emerge from these results. First, over the energy range shown, the single-particle

transition to $Ge^{+}4p$ has a much larger cross section than that of the two-particle transition to $Ge^{+}5s$. Second, we also note that, while generally good agreement between dipole-length and dipole-velocity results is seen for both cross sections, at the higher energies the length results start to oscillate. This is a numerical difficulty owing to the fact that the dipole-length formulation emphasizes the large-r region where the wave functions at high energy are less accurate than the intermediate-r region which is important for the dipole-velocity formulation. As a consequence, for still higher energies, we consider only the dipole-velocity form of the matrix element.

The calculated results going to 90,000 Ryd are shown for photoionization to $Ge^{+}4p$ and $Ge^{+}5s$ in FIGs. 3 and 4 respectives. Only dipole-velocity results are shown for reasons discussed above. The note-worthy point about these results is that, at the higher energies, $\sigma_{4p}$ is no longer much larger than $\sigma_{5s}$ - in fact they become comparable. This is in agreement with the derivation presented above that showed the $\sigma_{4p}$ decreases with increasing energy more rapidly than $\sigma_{5s}$. This can be seen more clearly in the ratio, $\sigma_{5s}/\sigma_{4p}$, shown in FIG.5. Here, at the higher energies, it is seen that the ratio increases linearly, as E. This shows that $\sigma_{4p}$ falls off more quickly than $\sigma_{5s}$ by just one power of E; exactly as our derivation predicted. As a matter of fact, at the highest energy considered, the ratio is more than 2, indicating that we have reached the

point where $\sigma_{5s}$ dominates; the two-electron transition dominates the single-electron transition.

To show that the case of Ge $4p^2$ photoionization is not an isolated one, analogous results are also presented for Sn $5p^2$ photoionization, leaving $Sn^+$ in the *5p* an *6s* states in FIG.6-10. Looking at these cross sections and ratios confirms entirely what was learned from the Ge case.

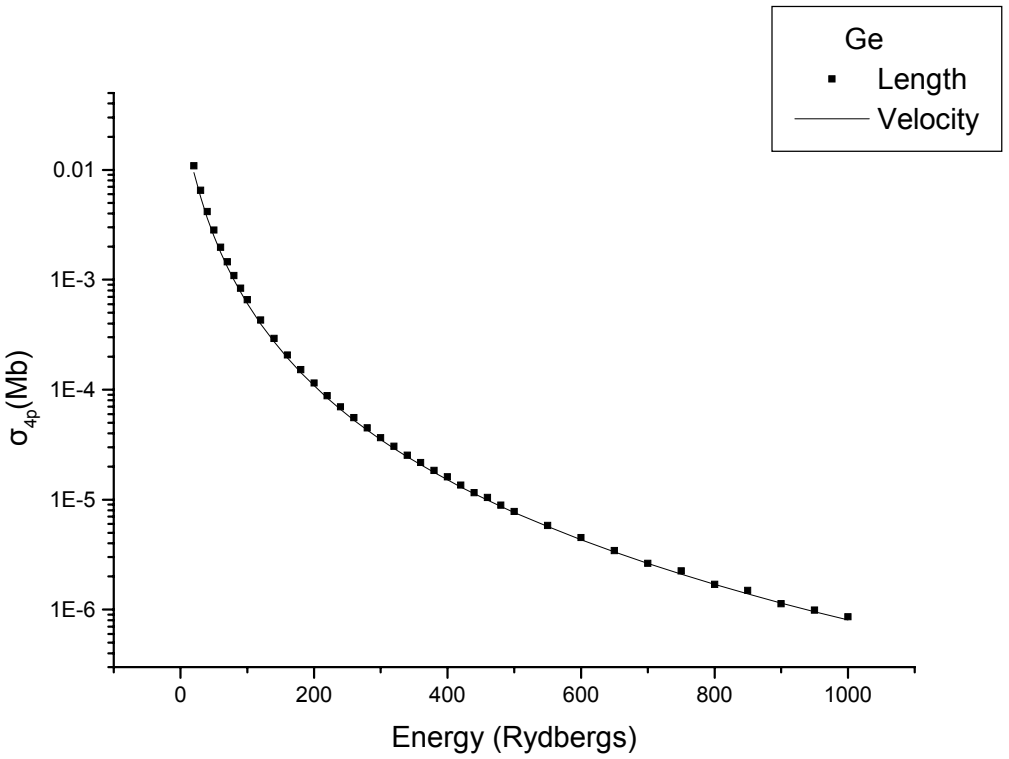


FIG.1 Photoionization cross section of Ge $4p^2\ ^1S$ leaving $Ge^+$ in the *4p* state in length and velocity formulation.

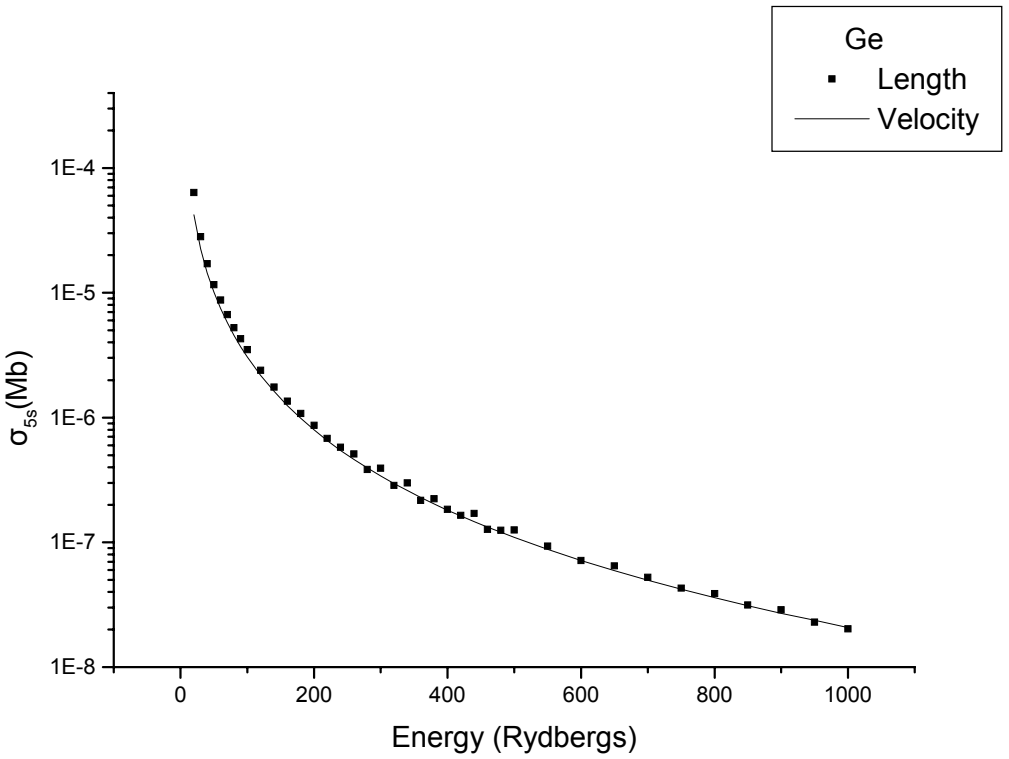


FIG.2 Photoionization cross section of Ge $4p^2\ ^1S$ leaving $Ge^+$ in the *5s* state in length and velocity formulation.

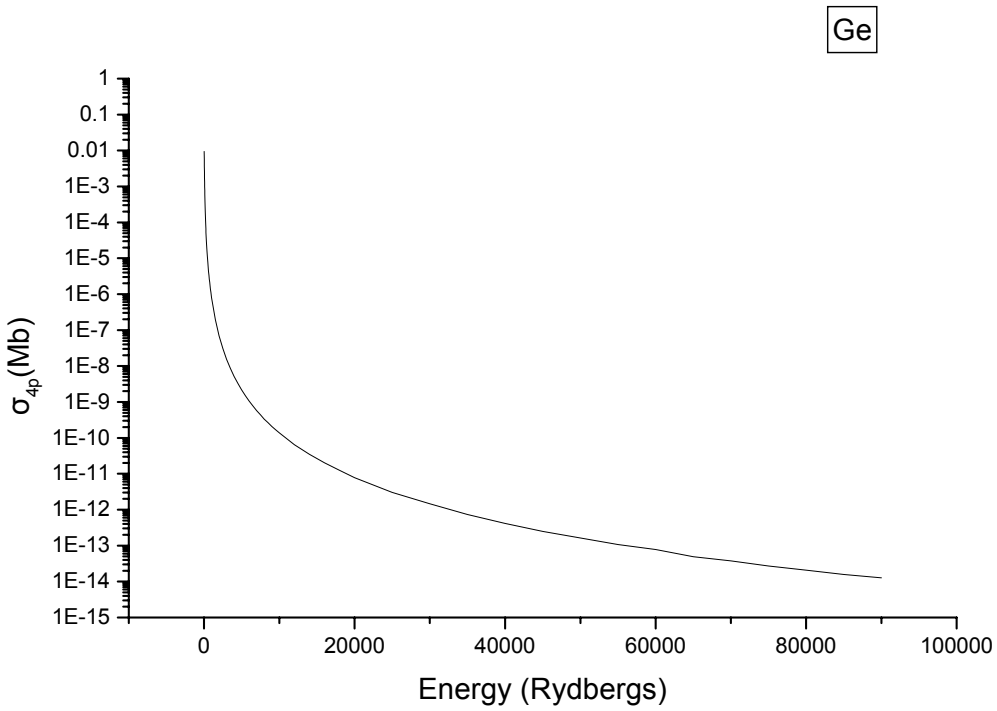


FIG.3 Photoionization cross section of Ge $4p^2$ $^1$S leaving $Ge^+$ in the *4p* state in velocity formulation.

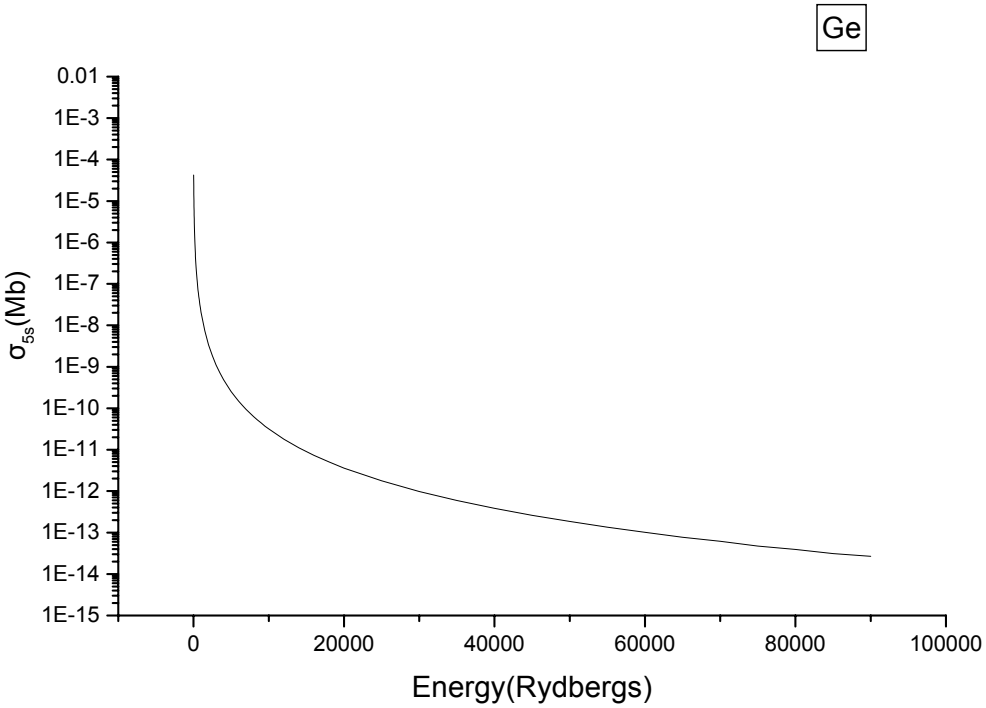


FIG.4 Photoionization cross section of Ge $4p^2$ $^1$S leaving $Ge^+$ in the *5s* state in velocity formulation.

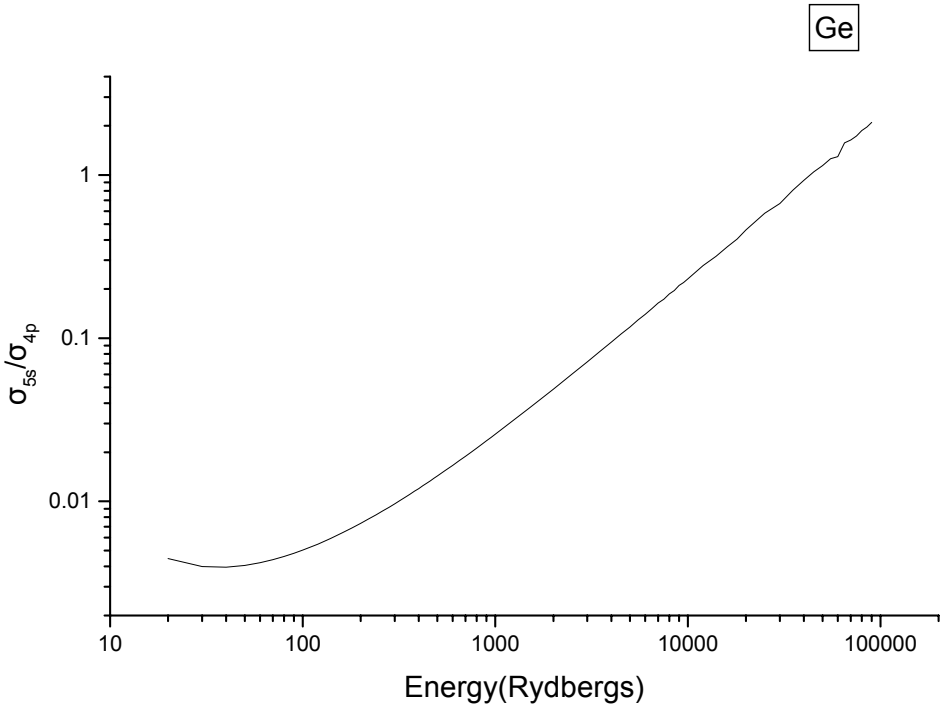


FIG.5 Ratio of photoionization cross section for $Ge^+$ *5s* production to $Ge^+$ *4p* production.

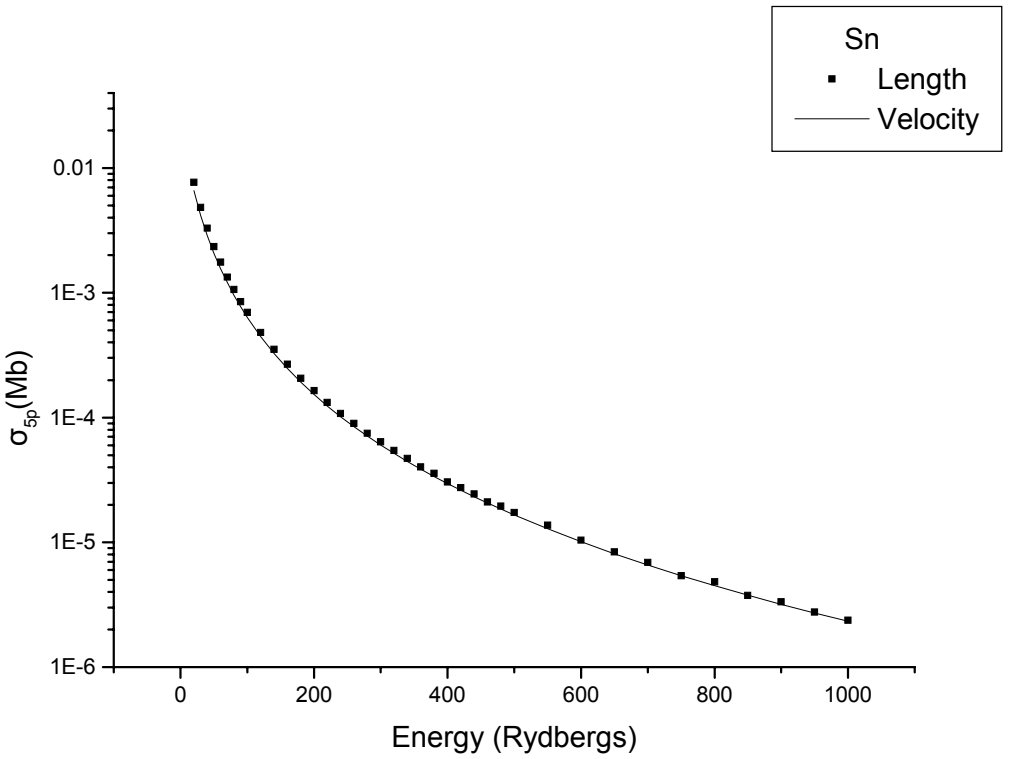


FIG.6 Photoionization cross section of Sn $5p^2\ ^1$S leaving $Sn^+$ in the *5p* state in length and velocity formulation.

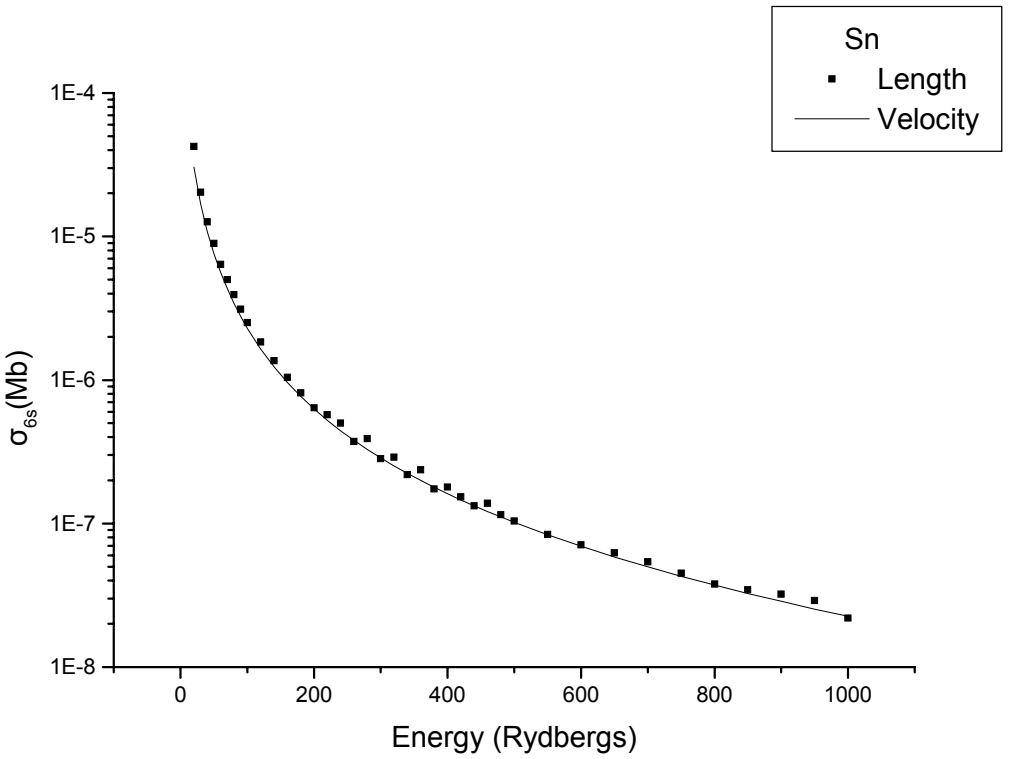


FIG.7 Photoionization cross section of Sn $4p^2\ ^1S$ leaving $Ge^+$ in the *6s* state in length and velocity formulation.

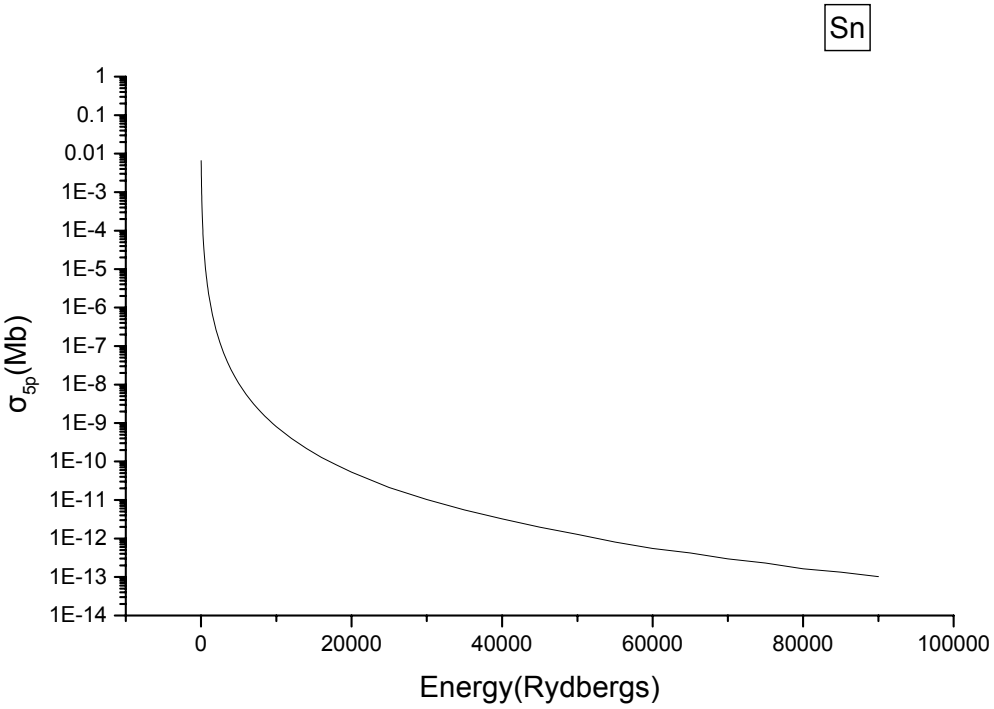


FIG.8 Photoionization cross section of Sn $5p^2$ $^1$S leaving $Sn^+$ in the *5p* state in velocity formulation.

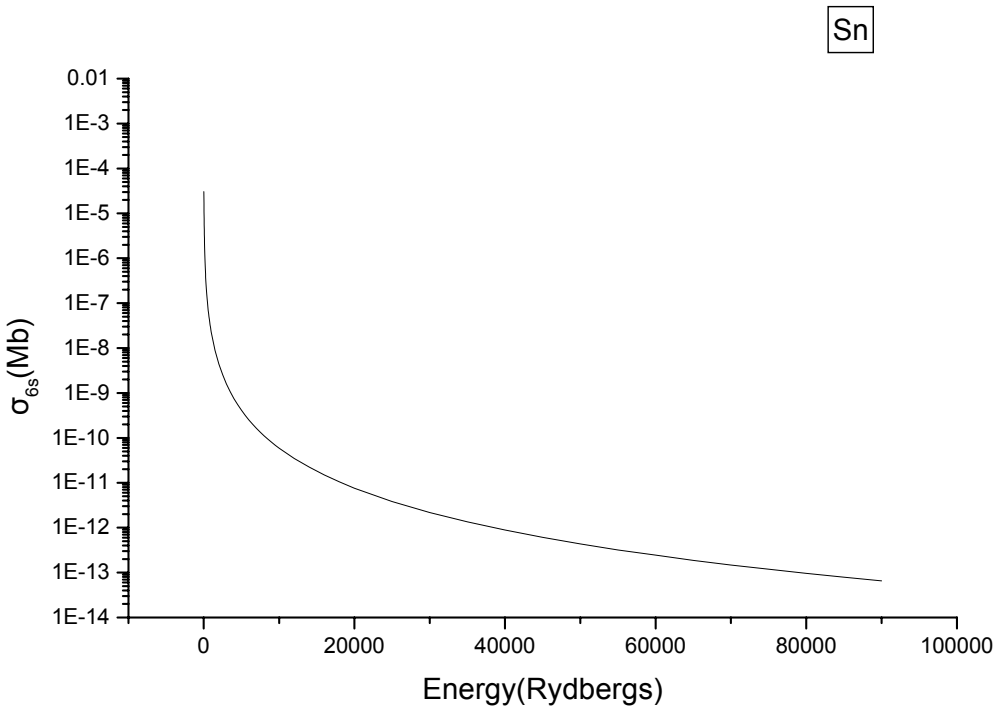


FIG.9 Photoionization cross section of Sn $5p^2$ $^1$S leaving $Sn^+$ in the *6s* state in velocity formulation.

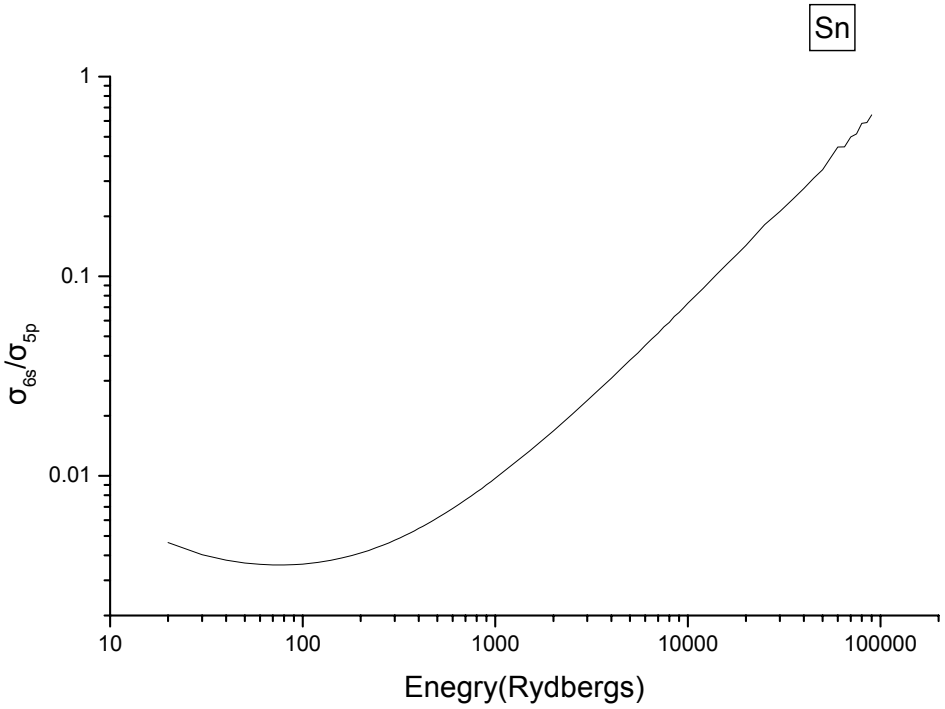


FIG.10 Ratio of photoionization cross section for $Sn^+$ *6s* production to $Sn^+$ *5p* production.

## 5. Conclusions

In this work we have derived the definitive result for the asymptotic high-energy dipole photoionization cross section/ oscillator strength, a problem that was thought to be solved in the 1930's. We have found that for almost all cases, the high-energy behavior is $E^{-7/2}$. Further, the dominant transition, at high energy, in almost all cases, is a satellite two-electron transition, photoionization plus excitation. Our theoretical predictions have been verified by direct calculation for Ge $4p^2$ and Sn $5p^2$ photoionization up to an energy of 90,000 Ryd. This is expected to be a general phenomenon over the entire periodic table.

## References

[1] M. Yan, H.R. Sadedhpour, and A. Dalgarno, Astrophys. J. **496**, 1044(1998).

[2] E.W.B. Dias, H.S. Chakraborty, P.C. Deshmukh, S.T. Manson, O. Hemmers, P. Glans, D.L. Hansen, H. Wang, S.B. Whitfield, D.W. Lindle, R. Wehlitz, J.C. Levin, I.A. Sellin, and R.C.C. Perera, Phys. Rev. Lett. **78**, 4553(1997).

[3] M.Ya. Amusia, N.B. Avdonina, E.G. Drukarew, S.T. Manson and R.H. Pratt, Phys. Rev. Lett. **85**, 4703(2000).

[4] U.Fano and A.R.P. Rau, Phys. Rev. **162**, 68(1967).

[5] G.N. Watson, A Treatise on the Theory of Bessel Functions (Cambridge Univ. Press, Cambridge, England, 1944), 2nd ed. (Formula used is Eq. (1), Sec. 13.24.)

[6] C. Froese Fischer, **The Hartree-Fock Method for Atoms** (John Wiley, New York, 1977) and references therein.